

Reconfigurable Balanced Dualband Bandstop Filter

Dubari Borah
 Dept. of Electrical and Computer Engineering
 University of Colorado, Colorado Springs
 Colorado Springs, USA
 dborah@uccs.edu

Thottam S. Kalkur
 Dept. of Electrical and Computer Engineering
 University of Colorado, Colorado Springs
 Colorado Springs, USA
 tkalkur@uccs.edu

Abstract—This paper introduces a novel architecture of reconfigurable balanced (differential) dualband bandstop filter (BSF). In differential mode (DM), each symmetrical bisection of the filter incorporates in-series cascade of two tunable dualband bandstop sections whereas high CMRR is achieved by loading open stubs to the symmetry plane of the branch line structure. To validate the proposed topology, a microstrip prototype is designed and fabricated. Both simulation and measured results show a good agreement with each other.

Keywords—Branchline structure, CM noise, CMRR, non-resonating node (NRN), tunable.

I. INTRODUCTION

Bandstop filter (BSF) is an important building block of modern communication system as it protects the transceiver from unwanted interference [1]. Recent development of communication systems with multiband services is attracting much attention for notch filters capable of producing multiple stopbands [2]. Furthermore, electronic industry is continuously striving for compact size for which reconfigurable circuitry is getting popular in both digital [3],[4] and analog applications [5],[6]. Because of this, the demand of multiband BSF with tunable response is growing rapidly for research and development.

Meanwhile, balanced topology is being widely employed in constructing microwave circuits and systems because they are more immune to signal noise than their single-ended counterparts. So far, researchers have investigated a variety of differential bandpass filter topologies [5] whereas significantly less work has been done in the field of differential BSF. In [1] and [7], CM noise of a single-band tunable balanced BSF has been suppressed by using magnetic field property of Substrate Integrated Waveguide (SIW) resonator and balanced property of double-sided parallel-strip line (DPSL), respectively. In [8] and [9], two balanced BSF structures employing one or more coupled line sections terminated with different loads are reported. In [6], a single-ended reconfigurable multiband BSF is reported. However, to the best of the author’s knowledge, no work has been published yet which applies differential topology to a dualband tunable BSF structure.

In this paper, a tunable balanced dualband BSF structure is proposed by integrating tunable dualband sections in a branch line structure. The high CMRR is obtained by using the properties of stepped impedance resonator (SIR).

II. PROPOSED DESIGN

Fig. 1 (a) shows the schematic of the proposed balanced dualband tunable BSF structure. This four-port branchline structure is symmetric about the horizontal central plane and each symmetrical bisection consists of two dualband sections connected in series through immittance inverter K_{12} . In each

dualband section, (θ_{L1}, Z_{L1}) and (θ_{L2}, Z_{L2}) are two quarter-wavelength lines at resonant frequencies f_1 and f_2 respectively and they are connected to the NRN (or NRN’) through inverters K_{01} and K_{02} , respectively. Both symmetrical bisections of the differential design are connected through tunable capacitors C_1 and C_2 in the central plane. Both NRN-NRN’ pairs share the open stubs (θ_{os1}, Z_{os1}) and (θ_{os2}, Z_{os2}) in the horizontal symmetry plane using K_{os} inverters for the flexible control of CM response. All the inverters are designed at the center frequency of the entire frequency spectrum, $(f_1 + f_2)/2$.

A. Differential Mode (DM) Operation

When the circuit in Fig. 1 (a) is excited by a differential signal, the horizontal symmetry plane acts as a perfect electric wall (Fig. 1 (b)). Therefore, the open stubs are short-circuited and have no effect on differential resonant frequencies. Note that the capacitor values C_1 and C_2 in Fig. 1 (a) become $2C_1$ and $2C_2$, respectively in DM operation.

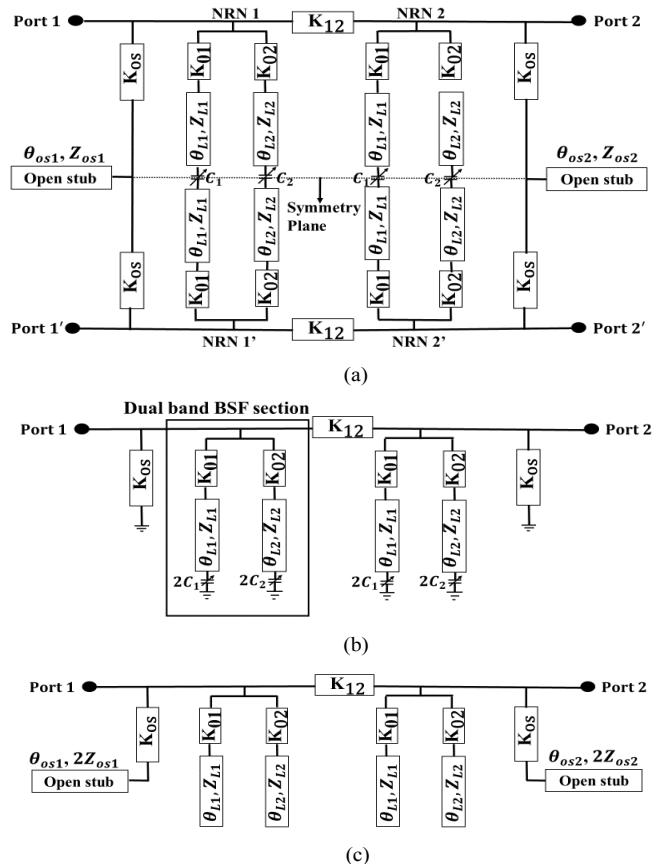


Fig. 1. (a) Schematic of the proposed topology, (b) DM equivalent circuit, and (c) CM equivalent circuit.

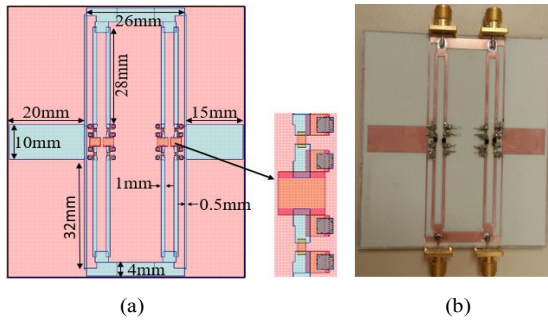


Fig. 2. (a) Layout of the design with zoomed version of the lumped element section and (b) fabricated prototype.

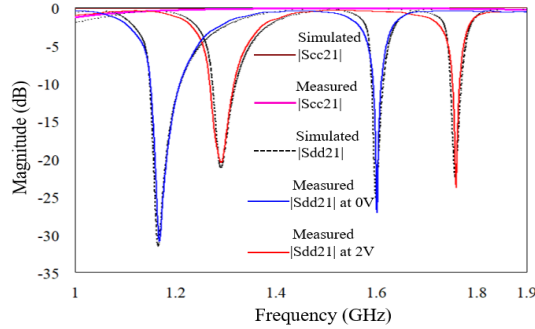


Fig. 3. DM insertion loss (Sdd21) and CM insertion loss (Scc21) plots of the proposed design.

B. Common Mode (CM) Operation

Under CM operation, the horizontal symmetry plane behaves as a perfect magnetic wall (Fig. 1 (c)). Therefore, the open stubs loaded in the symmetry plane cause extension and reconstruction of their corresponding couplings from the NRNs to form two SIRs. At resonance, each SIR produces two transmission zeros (TZs) [10]. By adjusting length and impedance of each open stub, the locations of the TZs can be controlled so that a flat CM bandpass response is achieved for each differential stopband, maintaining high CMRR.

III. RESULTS AND DISCUSSION

To validate the proposed topology, a microstrip line prototype is fabricated on Rogers RO4003 substrate with relative dielectric constant 3.38, dielectric thickness 1.52mm and dielectric loss tangent 0.0027 (Fig. 2). The two line-sections (θ_{L1} , Z_{L1}) and (θ_{L2} , Z_{L2}) are replaced by their equivalent low-pass π networks [11]. The π network for (θ_{L1} , Z_{L1}) consists of a series inductance of 3.6 nH (Coilcraft 0402CS series) and two shunt capacitances of 3 pF (ATC 100A series) each. Similarly, the π network for (θ_{L2} , Z_{L2}) consists of a series inductance of 1.4 nH (Coilcraft 0402CS series) and two shunt capacitances of 2 pF (ATC 100A series) each. Dimensions of the other line sections are presented in Fig. 2 (a). For both C_1 and C_2 , Skyworks SMV1233 model is used.

Fig. 3 shows that the measured response is in good agreement with the simulated response. The design is simulated using NI/AWR microwave office and the fabricated model is characterized with the help of Keysight N5224A 4-port network. From the Sdd21 plot, the tuning ranges of the

lower and upper stopbands are 1.16 GHz- 1.29 GHz and 1.6 GHz-1.76 GHz, respectively. The attenuation level of the lower stopband varies in the range of 20.5dB-30.7dB whereas for the upper stopband, it varies from 24dB to 26.7dB. The 3dB FBW of the lower band changes from 9% to 12% whereas the same for the upper band varies from 2.4% to 3.2%. Also, the Scc21 plot shows a flat 0 dB passband response which results in the minimum CMRR values of 20.5 dB and 24 dB for the lower stopband and the upper stopband, respectively.

IV. CONCLUSION

A novel topology of tunable balanced dualband BSF is proposed in this paper. Each DM bisection of this branch line structure consists of two dualband BSF sections separated by an impedance inverter. The CM noise is eliminated by loading the four-port differential structure with open stubs in the horizontal symmetry plane. Finally, the simulated response and the measured response are compared to show a good match with each other.

REFERENCES

- [1] M. F. Hagag, M. Abdelfattah, and D. Peroulis, "Balanced Octave-Tunable Absorptive Bandstop Filter," 2018 IEEE 19th Wireless and Microwave Technology Conference (WAMICON), Sand Key, FL, 2018, pp. 1-4.
- [2] D. Borah and T. S. Kalkur, "A Planar Multiband Balanced Bandstop Filter," 2018 IEEE MTT-S Latin America Microwave Conference (LAMC 2018), Arequipa, Peru, 2018, pp. 1-3.
- [3] S. N. Shahrouzi, "Optimized Embedded and Reconfigurable Hardware Architectures and Techniques for Data Mining Applications on Mobile Devices," Ph.D. Dissertation, University of Colorado Colorado Springs, December 2018.
- [4] S. N. Shahrouzi and D. G. Perera, "Dynamic partial reconfigurable hardware architecture for principal component analysis on mobile and embedded devices," EURASIP Journal on Embedded Systems, Springer Open, vol. 2017, article no. 25, Feb. 2017.
- [5] D. Borah and T. S. Kalkur, "A Balanced Dual-band Tunable Bandpass Filter," 2018 International Applied Computational Electromagnetics Society Symposium (ACES), Denver, CO, 2018, pp. 1-2.
- [6] D. Psychogiou, R. Gomez-Garcia, and D. Peroulis, "A class of fully-reconfigurable planar multi-band bandstop filters," 2016 IEEE MTT-S International Microwave Symposium (IMS), 2016.
- [7] J. Cai, Y. J. Yang, W. Qin, and J. X. Chen, "Wideband Tunable Differential Bandstop Filter Based on Double-Sided Parallel-Strip Line," in IEEE Transactions on Components, Packaging and Manufacturing Technology.
- [8] M. Kong, Y. Wu, Z. Zhuang, and Y. Liu, "Narrowband balanced absorptive bandstop filter integrated with wideband bandpass response," in Electronics Letters, vol. 54, no. 4, pp. 225-227, February 22 2018.
- [9] J. Sorocki, I. Piekarczyk, S. Gruszczynski, and K. Wincza, "Low-Loss Directional Filters Based on Differential Band-Reject Filters With Improved Isolation Using Phase Inverter," in IEEE Microwave and Wireless Components Letters, vol. 28, no. 4, pp. 314-316, April 2018.
- [10] M. Sagawa, M. Makimoto, and S. Yamashita, "Geometrical structures and fundamental characteristics of microwave stepped-impedance resonators," IEEE Transactions on Microwave Theory and Techniques, vol. 45, no. 7, pp. 1078-1085, July 1997.
- [11] M. M. Elsbury, P. D. Dresselhaus, N. F. Bergren, C. J. Burroughs, S. P. Benz, and Z. Popovic, "Broadband Lumped-Element Integrated N-Way Power Dividers for Voltage Standards," in IEEE Transactions on Microwave Theory and Techniques, vol. 57, no. 8, pp. 2055-2063, Aug. 2009.